Ser165 in the Second Transmembrane Region of the Kir2.1 Channel Determines its Susceptibility to Blockade by Intracellular Mg^{2+}

Yuichiro Fujiwara[1] and Yoshihiro Kubo[1,2]

[1]Department of Physiology and Cell Biology, Tokyo Medical and Dental University Graduate School and Faculty of Medicine, Tokyo 113-8519, Japan

[2]CREST, Japan Science and Technology Corporation, Saitama 332-0012, Japan

ABSTRACT The strong inward rectification of Kir2.1 currents is reportedly due to blockade of the outward current by cytoplasmic magnesium (Mg^{2+}_i) and polyamines, and is known to be determined in part by three negatively charged amino acid residues: Asp172, Glu224, and Glu299 (D172, E224, E299). Our aim was to identify additional sites contributing to the inward rectification of Kir2.1 currents. To accomplish this, we introduced into wild-type Kir2.1 and its D172N and D172N & E224G & E299S mutants various point mutations selected on the basis of a comparison of the sequences of Kir2.1 and the weak rectifier sWIRK. By analyzing macroscopic currents recorded from *Xenopus* oocytes using two-electrode voltage clamp, we determined that S165L mutation decreases inward rectification, especially with the triple mutant. The susceptibility to blockade by intracellular blockers was examined using HEK293 transfectants and the inside-out patch clamp configuration. The sensitivity to spermine was significantly diminished in the D172N and triple mutant, but not the S165L mutant. Both the S165L and D172N mutants were less susceptible to blockade by Mg^{2+}_i than the wild-type channel, and the susceptibility was still lower in the D172N & S165L double mutant. These results suggest that S165 is situated deeper into the pore from inside than D172, where it is accessible to Mg^{2+}_i but not to spermine. The single channel conductance of the D172N mutant was similar to that of the wild-type Kir2.1, whereas the conductance of the S165L mutant was significantly lower. Permeation by extracellular Rb^+ (Rb^+_o) was dramatically increased by S165L mutation, but was increased only slightly by D172N mutation. By contrast, the Rb^+/K^+ permeability ratio was increased equally by D172N and S165L mutation. We therefore propose that S165 forms the narrowest part of the Kir2.1 pore, where both extracellular and intracellular blockers plug the permeation pathway.

KEY WORDS: inward rectification • mutation • structure and function • inside-out patch clamp • Kir2.1

INTRODUCTION

Inward rectification of outward currents through the Kir2.1 inwardly rectifying K^+ channel is reportedly due to blockage by cytoplasmic Mg^{2+} (Matsuda et al., 1987; Vandenberg, 1987; Matsuda, 1988) and polyamines (Ficker et al., 1994; Lopatin et al., 1994; Fakler et al., 1995; Ishihara et al., 1996; Nichols and Lopatin, 1997). Three negatively charged amino acid residues that affect this inward rectification have been identified. The first identified was D172, which is situated in the M2 transmembrane region of Kir2.1 (Fig. 1 A). A D172N Kir 2.1 mutant showed reduced susceptibility to blockade by both cytoplasmic polyamines and Mg^{2+}_i (Lu and MacKinnon, 1994; Stanfield et al., 1994; Wible et al., 1994). The second site identified was E224, which is situated in the putative cytoplasmic chain after M2 (Taglialatela et al., 1995; Yang et al., 1995). Finally, we recently identified a third site, E299, which is situated about midway through the putative cytoplasmic chain following the M2 region. This site influences particularly the susceptibility to blockade by spermine (Kubo and Murata, 2001).

We also observed that an E176Q mutant of the sWIRK salmon weakly inwardly rectifying K^+ channel, which contains no negative charges at sites corresponding to the aforementioned three (E176Q & G228 & S308), showed no clearly detectable inward rectification (Kubo et al., 1996). On the other hand, weak but clear inward rectification remained in the triple Kir2.1 mutant D172N & E224G & E299Q, which also has no negative charges at the indicated sites (Kubo and Murata, 2001). Thus, the difference in the intensities of the inward rectification of currents through Kir2.1 and sWIRK cannot be entirely explained by differences in these three sites. We therefore postulated the presence of one or more additional sites that contribute to the inward rectification.

One aim of the present study was to identify other site(s) that affect the inward rectification of currents through Kir2.1. To accomplish this, we made various mutants based on the comparison of the amino acid se-

Address correspondence to Yoshihiro Kubo, Department of Physiology and Cell Biology, Tokyo Medical and Dental University, Graduate School and Faculty of Medicine, 1-5-45 Yushima, Bunkyo-ku, Tokyo 113-8519, Japan. Fax: (81) 3-5803-5156; E-mail: ykubo.phy2@med.tmd.ac.jp

TABLE I

Screening for Inward Rectification Properties of Mutants

	No alteration of rectification	No functional currents
N-cytoplasmic region	G65R, A70R, A70K, A70S, R74A R80Q	C54S, D71E, D78E
Pore region	A91T, V93I, V93T, F163V, I166V, G168T, I176T	S136F
C-cytoplasmic region	K223Q, I201V, L231E, S238K, E293Q, A306S, R325E, E333S, D340K, E349K, K362E, E387	L217E, E303K, E303Q, G300V

The amino acid sequence of Kir 2.1 was compared with that of sWIRK. To survey critical sites for inward rectification, these point mutants were made in the wild-type and D172N & E224G & E299Q triple mutant of Kir 2.1.

quences of Kir2.1 and sWIRK (Table I). We observed that S165L mutation of a D172N & E224G & E299Q triple Kir2.1 mutant markedly weakened inward rectification, and therefore focused on S165, which is located in M2 region (Fig. 1, A and B). In that regard, Thompson et al. (2000) reported that the same S165L mutation of Kir2.1 reduced the susceptibility to blockade by extracellular Rb^+ and Cs^+ and dramatically increased Rb^+ permeance. In that context, our results suggest that the same site affects the susceptibility to blockade by cations from both the intracellular and extracellular sides.

Although the pore structure of the KcsA channel has been resolved by X-ray crystallography (Doyle et al., 1998), whether this finding is applicable to the Kir2.1 inward rectifier is controversial (Minor et al., 1999; Thompson et al., 2000). Therefore, a second aim of this study was to glean useful information about the inward rectification mechanism and about the inner pore structure of Kir 2.1 from data related to the affinities of intracellular and extracellular blockers.

MATERIALS AND METHODS

In Vitro Mutagenesis

The single point mutants were made with a QuickChange site-directed mutagenesis kit (Stratagene) or a Sculptor in vitro mutagenesis kit (Amersham Biosciences) using mutated oligonucleotide DNA primers and single stranded mouse wild-type Kir2.1 ssDNA. The introduction of a mutation was confirmed by sequencing with a BigDye terminator sequencing kit (Applied Biosystems) and an automatic DNA sequencer (ABI type 377, ABI type 310). The electrophysiological properties of two independent mutant clones were confirmed to be identical. The double-point mutants were made using the ssDNA of the single-point mutants, the triple mutants were prepared using the ssDNA of the double mutants, and quadruple-point mutants were prepared using the ssDNA of the triple-point mutants.

Two-electrode Voltage Clamp Recordings in Xenopus Oocytes

Xenopus oocytes were collected from frogs anesthetized in water containing 0.15% tricaine; after the final collection the frogs were killed by decapitation. Isolated oocytes were treated with collagenase (2 mg/ml, type 1; Sigma-Aldrich) and then injected with ~50 nl of cRNA solution prepared from the linearized plas-

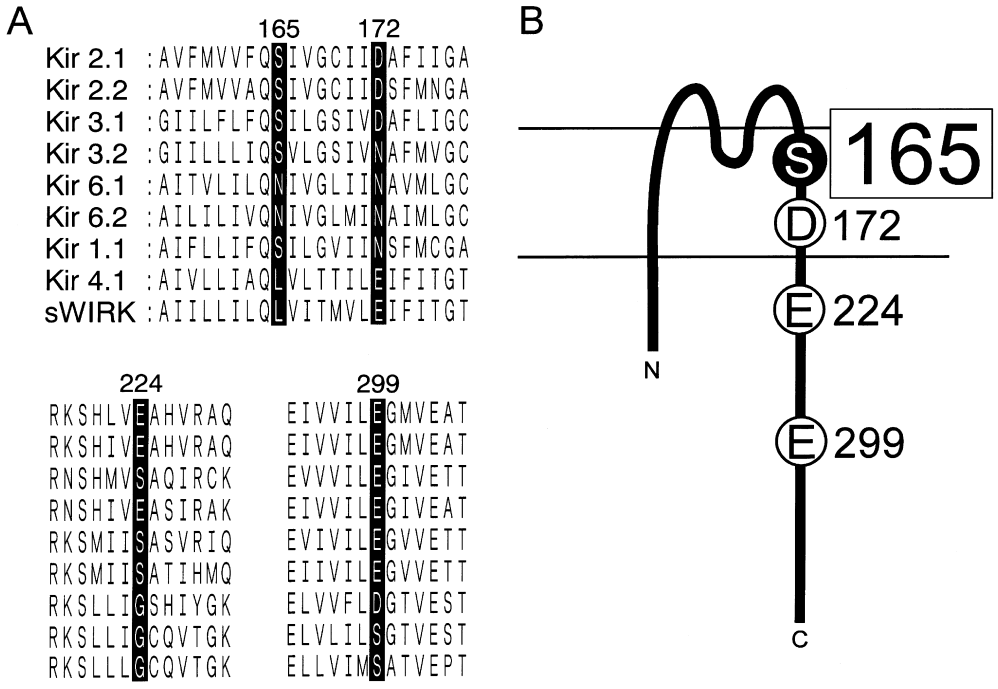

FIGURE 1. Conservation of four amino acid residues critical for inward rectification among the inward rectifier K^+ channel family. (A) Alignment of the amino acid sequences of the inwardly rectifying K^+ channel family at D172, E224, E299, and E165 of Kir2.1 and the surrounding region. The original reports used for the alignment are as follows. Kir 2.1 (Kubo et al., 1993a), Kir 2.2 (Koyama et al., 1994), Kir 3.1 (Kubo et al., 1993b), Kir 3.2 (Lesage et al., 1994), Kir 6.1 (Inagaki et al., 1995a), Kir 6.2 (Inagaki et al., 1995b), Kir 1.1 (Ho et al., 1993), Kir 4.1 (Bond et al., 1994; Takumi et al., 1995), and sWIRK (Kubo et al., 1996). (B) Schematic diagram of the structure of Kir2.1 based on the initial model by Kubo et al. (1993a). Both D172 and S165L are located within the α-helix of the second transmembrane region (M2). E224, situated just after M2, and E299, situated at the center of the putative cytoplasmic chain after M2, are also depicted.

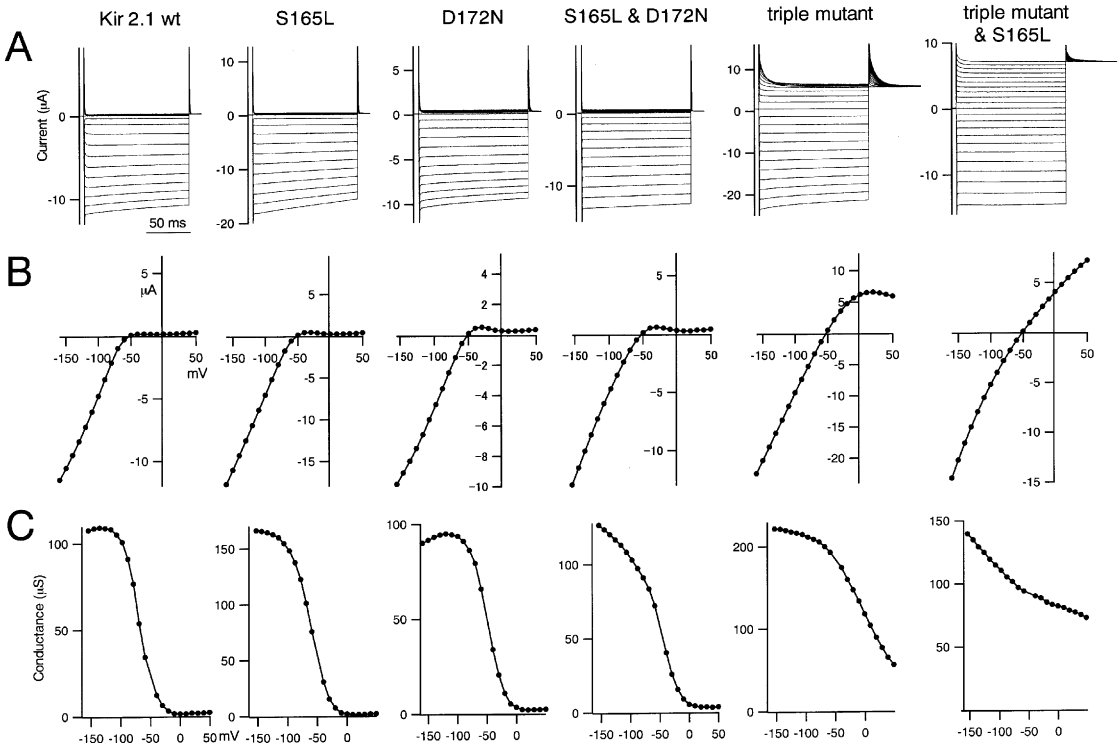

FIGURE 2. Comparison of macroscopic currents through wild-type and mutant Kir2.1 expressed in *Xenopus* oocytes. (A) Macroscopic currents recorded using two-electrode voltage clamp with *Xenopus* oocytes expressing wild-type Kir2.1 or S165L, D172N, D172N, & S165L double mutant, D172N & E224G & E299S triple mutant, or triple mutant & S165L. Representative current traces recorded in 10 mM K^+_o. The holding potential was −50 mV; step pulses from 50 to −160 mV were applied in 10-mV decrements. (B) I-V relationships for the data in A; values were measured 50 ms after the onset each step pulse. (C) Conductance-voltage (G-V) relationship for the data in B.

mid DNA using an RNA transcription kit (Stratagene). The injected oocytes were incubated for 2–4 d at 17°C in frog Ringer solution (Kubo et al., 1993a) supplemented with 20 mM KCl.

Macroscopic currents were recorded in the two-electrode voltage clamp configuration using a bath-clamp amplifier (OC-725C; Warner Co.). Stimulation, data acquisition, and analysis were done on a Pentium-based computer using Digidata 1322A and pCLAMP software (Axon Instruments, Inc.). Intracellular glass microelectrodes were filled with 3 M potassium acetate with 10 mM KCl (pH 7.2). The microelectrode resistances ranged from 0.1 to 0.3 MΩ. Two Ag-AgCl pellets (Warner Co.) were used to pass the bath current and sense the bath voltage. The voltage-sensing electrode was placed near the oocyte (~2 mm away), on the same side as the voltage-recording microelectrode. The bath current–passing pellet and the current injection microelectrode were placed on the other side. Under these conditions, the series resistance between the oocyte surface and the bath voltage-sensing pellet was ~200 Ω (Sabirov et al., 1997). As the measured current at the most hyperpolarized potential was 35 μA in the largest case, and was mainly <20 μA, the voltage-clamp error due to this series resistance was estimated to be no more than 7 mV and mostly <4 mV. This error, which was not compensated in the experiments, did not change the conclusions drawn from the comparison of wild-type and mutant channels.

All recordings in this work were performed at room temperature (20–23°C). For the data summarized in Figs. 2–4 and 9 A, the recording bath solution contained 10 mM KCl, 80 mM *N*-methyl-glucamine, 70 mM HCl, 3 mM $MgCl_2$, and 10 mM HEPES, pH 7.4. For the data on Rb^+ permeance in Fig. 9 B, the recording bath solution contained 10 mM RbCl, 80 mM *N*-methyl-glucamine, 70 mM HCl, 3 mM $MgCl_2$, and 10 mM HEPES, pH 7.4. By assuming an intracellular potassium concentration ($[K^+]_i$) of 80 mM, the E_K was calculated to be −52 mV; however, the exact values of $[K^+]_i$ and E_K for each oocyte are unknown. The E_K used for the calculation of the chord conductance (Figs. 2 and 3) was therefore adjusted to yield a continuous G-V plot. The adjusted E_K ranged from −54 to −49 mV.

Leak subtraction was not done in this study. It is critical to avoid the contamination of leak component to discuss the intensity of inward rectification. Therefore, we avoided setting E_K to zero mV, in which case the discrimination between outward Kir current and leak component is hard. We instead used a mixture of K^+ and *N*-methyl-glucamine (NMG)* as extracellular solution to set E_K at e.g., −50 mV. We carefully monitored the reversal potential during the recordings, and judged that the leak level was ignorable when the cells showed expected reversal potential. Only data which satisfied these criteria were used for the analysis.

Data from the same batch of oocytes were used for comparison of phenotypes (Figs. 2–4 and 9) because properties such as inward rectification and blocking speed, which are influenced by the cytoplasmic polyamine concentration, differ significantly from batch to batch. Nevertheless, similar tendencies were reproducibly observed in five batches of oocytes.

**Abbreviations used in this paper:* GFP, green fluorescent protein; NMG, *N*-methyl-glucamine.

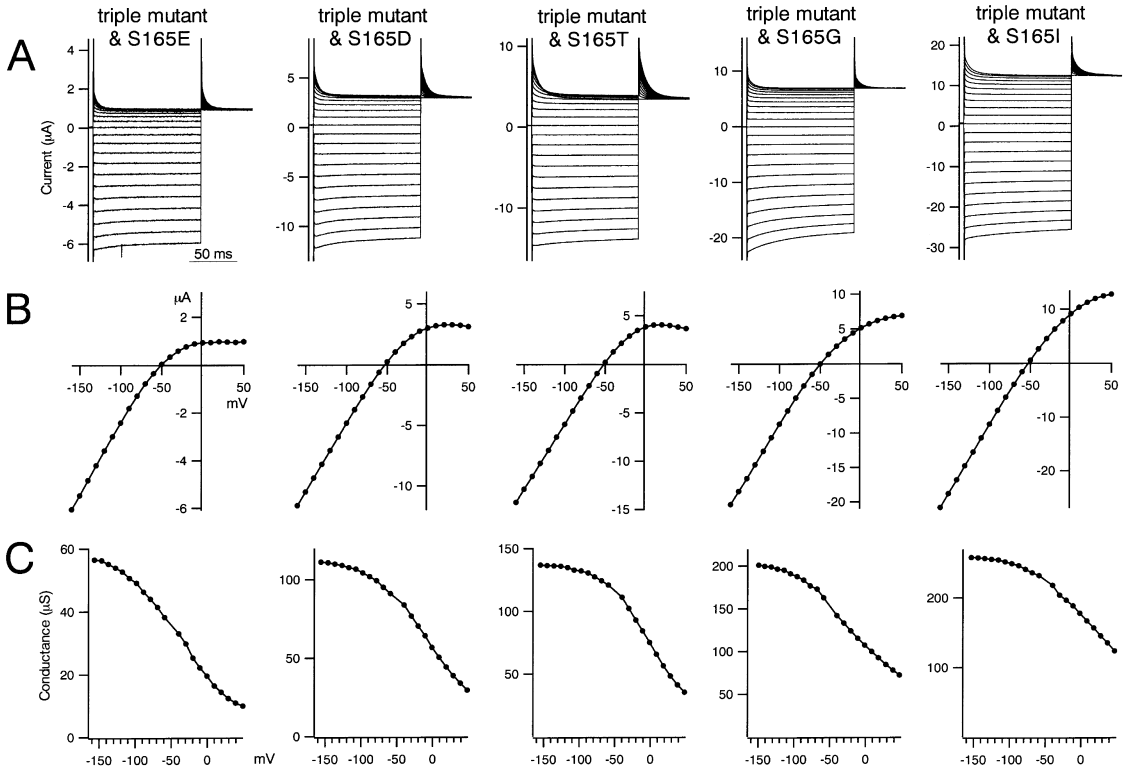

FIGURE 3. Macroscopic currents recorded by two-electrode voltage-clamp of *Xenopus* oocytes expressing various mutants in which S165 in the D172N & E224G & E299Q triple Kir2.1 mutant was substituted with E, D, T, G, or L. The data were recorded and analyzed as in Fig. 2.

Single-channel Recordings in Xenopus Oocytes

For single-channel recording, the vitelline membrane was peeled off by bathing the oocytes for 5–10 min in a hyperosmolar solution (Kubo et al., 1993a). The patch pipettes were prepared from borosilicate glass (Warner Instruments) using a P-97 horizontal puller (Sutter) and a fire polisher (Narishige). Pipette resistance ranged from 4 to 9 MΩ. Recordings were obtained under the cell-attached configuration using an AxoPatch 1D amplifier (Axon Instruments, Inc.). The recorded currents were low pass filtered at 1 kHz using a Bessel filter built into the amplifier and digitized at 5 kHz. The recordings shown in Fig. 12 A were digitally filtered at 500 Hz. The pipette (extracellular) and bath solutions contained 136 mM KCl, 3 mM $MgCl_2$, 10 mM HEPES, and 4 mM KOH, pH 7.4.

Expression in HEK293T Cells

The cDNAs for wild-type and mutant Kir2.1 were subcloned into the pCXN2 expression vector (Niwa et al., 1991). The plasmid DNA was then cotransfected into HEK293T cells (human embryonic kidney cell line) along with a transfection marker, enhanced green fluorescent protein (GFP) (CLONTECH Laboratories, Inc.; 1/15 the amount of plasmid DNA), using Lipofectamine Plus (GIBCO BRL) as instructed by the manufacturer. The cells were cultured in Dulbecco's modified Eagle's medium with 10% bovine calf serum for 24 h. The transfectants were then dissociated by treatment with 0.025% trypsin in Ca^{2+}- and Mg^{2+}-free PBS, and reseeded on coverslips at a relatively low density. The reseeding was done to obtain well-isolated cells and to facilitate successful giga-ohm seal formation. Prior to experimentation, we confirmed that the trypsin treatment did not change the electrophysiological properties of the expressed channels. Electrophysiological recordings were performed 7–24 h after reseeding, which corresponds to 18–35 h after transfection.

Macroscopic Current Recordings in HEK293T Cells

A coverslip with HEK293T cells was placed in a recording chamber containing bath solution (see below) on the stage of an inverted fluorescence microscope (IX70; Olympus), and the transfected cells were identified by the fluorescent signal of the cotransfected GFP. Macroscopic currents were then recorded in the excised inside-out patch configuration using an Axopatch-1D amplifier. The resistance of the patch pipettes ranged from 2 to 4 MΩ. 50–80% of the voltage error due to the series resistance was compensated by a circuit in the amplifier. The level of expression achieved with the combination of HEK293T cells and the $pCXN_2$ expression was sufficient for macroscopic current recording using standard-sized patch pipettes. The recorded currents were low-pass filtered at 1 kHz by a circuit built into the amplifier.

The pipette (extracellular side) solution contained 16 mM KCl, 120 mM NMG, 102 mM HCl, 3 mM $MgCl_2$, 10 mM HEPES, and 4 mM KOH, pH 7.4 (Figs. 5–8 and 10 A), or 16.6 mM RbCl, 120 mM NMG, 102 mM HCl, 3 mM $MgCl_2$, 10 mM HEPES and 3.4 mM RbOH (pH 7.4) (Fig. 10 B). The bath (intracellular side) solution containing various concentrations of Mg^{2+} or spermine was prepared as described by Ishihara et al. (Ishihara et al., 1996) with some modifications. We used KH_2PO_4 and K_2HPO_4 as a pH buffer because HEPES, or some accompanying impurity, reportedly causes inward rectification (Guo and Lu, 2000). Mg^{2+}- and spermine-free solution contained 116.88 mM KCl, 2 mM EDTA, 2.83 mM KH_2PO_4, 7.17 mM K_2HPO_4, and 5.95 mM KOH (pH

7.2). $MgCl_2$ was added to adjust the free Mg^{2+} concentration; the amount added was calculated using the free software Sliders v2.00 (Chris Patton, Stanford University, http://www.stanford.edu/~cpatton/maxc.html). The amounts of added $MgCl_2$ and the (free Mg^{2+}) concentration were: 1.06 mM (3.00 μM), 1.87 mM (30.5 μM), 2.28 mM (298 μM), and 5 mM (3 mM). The acidic shift in pH caused by adding $MgCl_2$ was adjusted to pH 7.2 by applying KOH, and the total K^+ concentration was adjusted to 140 mM. Spermine (Sigma-Aldrich) was simply added to the solution just before the experiments, and solutions containing spermine were used for up to 2 h. The concentration of added spermine is indicated in Figs. 7–8. The total $[K^+]_o$ and $[K^+]_i$ were ~20 and 140 mM. The liquid junction potential between the pipette solution and the bath solution was ~11 mV (Figs. 5–8 and 10 A) or 8 mV (Fig. 10 B); membrane potentials were corrected for this value.

The degree of run-down that occurred during acquisition of the recordings used for determining I-V relationships was monitored by reapplying the step pulses, and data with apparent run-down were discarded. Given this limitation, it was not possible to obtain data for all concentrations of the blockers from one patch, and the data shown in Figs. 5–8 were obtained from multiple patches. In addition, it was very difficult to wash out cytoplasmic polyamines, so recordings were started after perfusing the bath (intracellular side) for 15–30 min.

Cysteine-scanning Mutagenesis

The accessibility of cys-modifying reagents from extracellular side was analyzed as we described previously (Kubo et al., 1998) using *Xenopus* oocytes under two-electrode voltage clamp. The bath solution contained 24 mM KCl, 66 mM N-methyl-glucamine, 42 mM HCl, 3 mM $MgCl_2$, and 5 mM HEPES pH 7.4 (Fig. 13 A). By assuming an intracellular potassium concentration ($[K^+]_i$) of 80 mM, the E_K was calculated to be −30 mV. The accessibility from intracellular side was analyzed as described by Lu et al. (1999) using transfected HEK293 cells by inside-out patch clamp macroscopic current recording. The pipette (extracellular) and the bath (intracellular) solution with no Mg^{2+} and spermine was the same as those used in Figs. 5–8. Cys-modifying reagents, 2-trimethylammonium ethyl methane-thiosulfonate bromide (MTSET; Toronto Research) and 2-aminoethyl methane-thiosulfonate bromide (MTSEA; Toronto Research) were dissolved in the bath solution just before use, and one-fifth volume of five times the concentrated stock solution of them or Cd^{2+} was applied to the bath and was mixed immediately through pipetting.

RESULTS

The S165L Mutation Weakened Inward Rectification

We aimed to identify amino acid residues other than D172, E224, and E299 that contribute to the inward rectification of currents through Kir2.1. We focused chiefly on negatively charged amino acid residues D and E, and on S or T, which are present in Kir 2.1 and other strong inward rectifiers, but not in sWIRK. These amino acids were mutated one at a time (Table I) in wild-type Kir 2.1 and in the D172N & E224G & E299Q triple mutant. This systematic analysis revealed that, in most cases, mutation either induced unremarkable changes in the inward rectification or made the channel nonfunctional (Table I). We chose to focus on

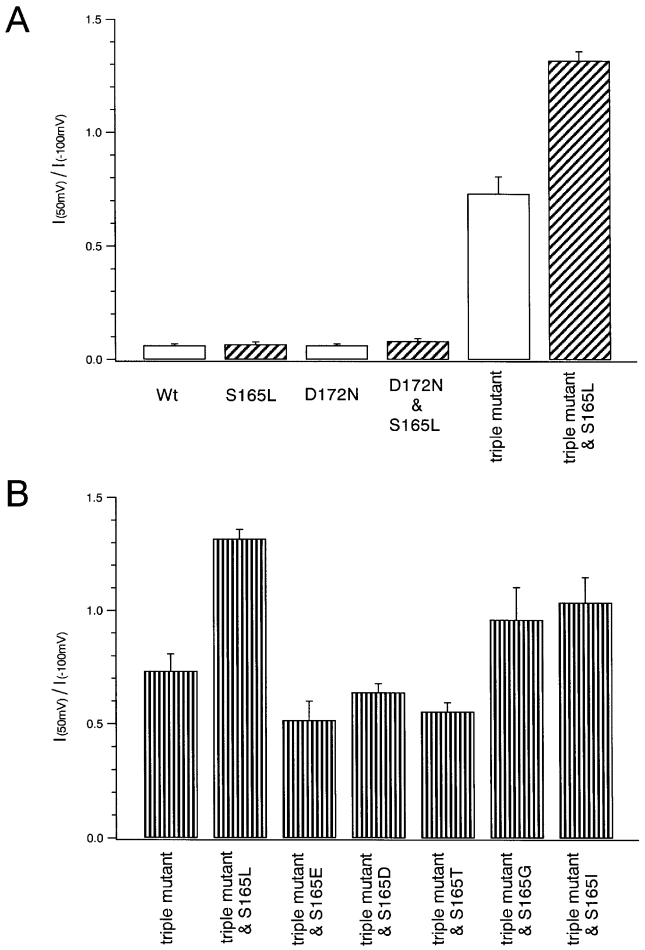

FIGURE 4. Inward rectification of currents through wild-type and mutant Kir2.1. (A and B) The ratios of the current amplitudes measured 50 ms after the onset of step pulses to 50 and −100 mV were calculated as an index of rectification intensity. Bars depict means ± SD (n = 4 of each group). A and B reflect the data shown in Figs. 2 and 3, respectively.

mutation of S165, which is located in the M2 region (Fig. 1).

Initially, the electrophysiological effects of S165L mutation on wild-type Kir2.1 and its D172N and D172N & E224G & E299Q triple mutants were compared (Fig. 2). Macroscopic currents recorded in 10 mM K^+ using two-electrode voltage clamp in *Xenopus* oocytes are shown in Fig. 2 A; also shown are the I-V (Fig. 2 B) and G-V (Fig. 2 C) relationships. As an index of the intensity of the inward rectification, the ratios of the current amplitudes at 50 and −100 mV were calculated (Fig. 4 A).

S165L mutation did not affect the inward rectification of currents through the wild-type channel remarkably. The I-V relationship for the D172N mutant showed a notable outward hump, and rectification was weaker than in the wild-type channel. Introduction of the S165L mutation into the D172N mutant did not substantially

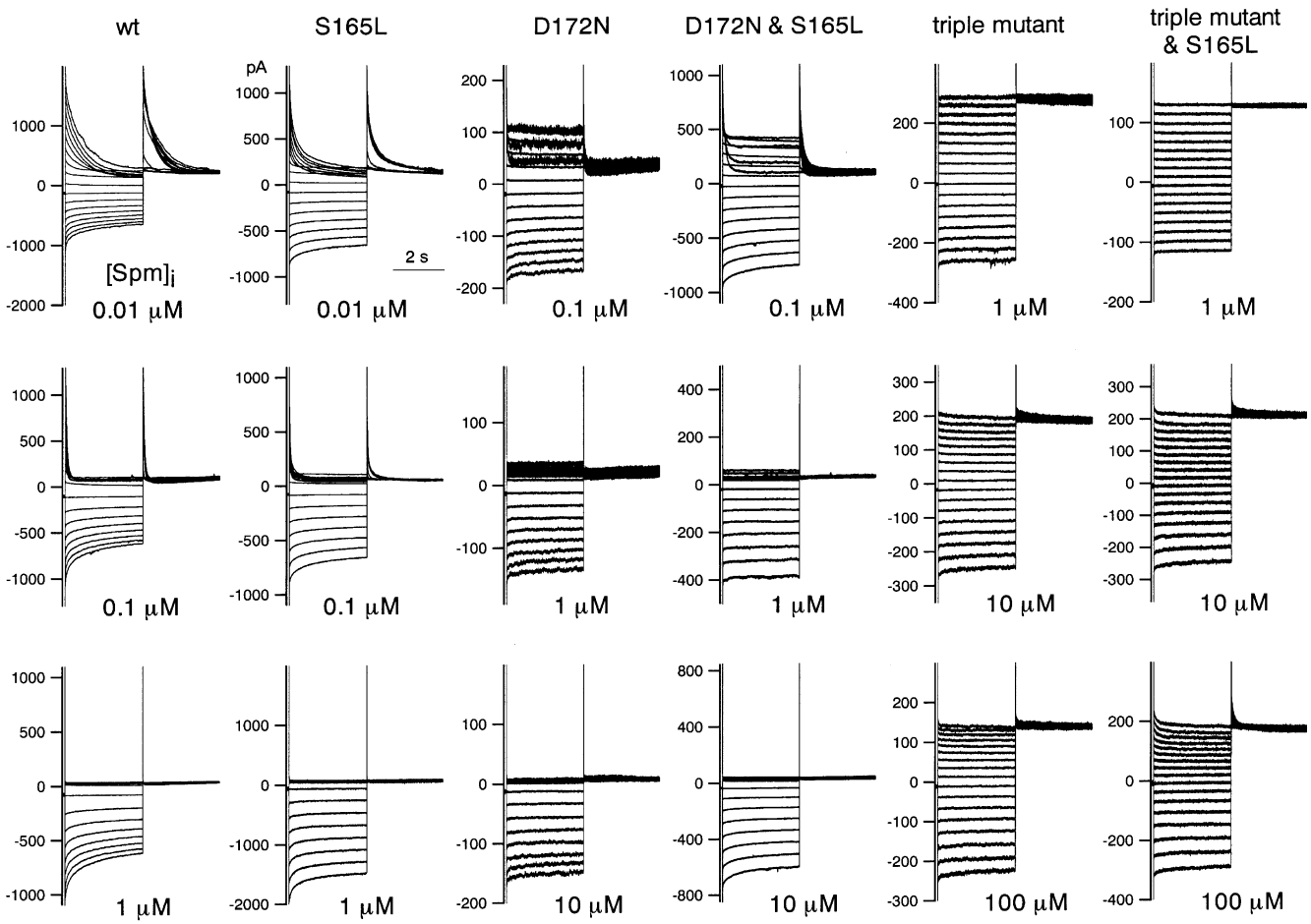

FIGURE 5. Macroscopic currents recorded in the presence of the indicated concentrations of spermine from excised patches of HEK293T cells expressing wild-type or mutant Kir2.1. Note the difference in concentration ranges used for wild-type and S165L (0.01, 0.1, and 1 μM), D172N and D172N & S165L (0.1, 1, and 10 μM), and D172N & E224G & E299Q and D172N & E224G & E299Q & S165L (1, 10, and 100 μM) channels. K^+_o and K^+_i were 20 and 140 mM, respectively. The holding potential was −50 mV, and step pulses from 40 to −120 mV were applied in 10-mV decrements.

alter these findings. The D172N & E224G & E299S triple mutant showed a large outward current and significantly weakened rectification. Moreover, addition of the S165L mutation decreased the inward rectification still further, so that large outward currents were observed even at the most depolarized potentials (Fig. 2 A). These results suggest that S165 is a key determinant of the strength of the inward rectification of currents through Kir2.1, but its significance is masked in the presence of E224 and E299, which mediate strong rectification.

It was also notable that the S165L mutation affected the G-V relationship at hyperpolarized potentials (Fig. 2 C). The conductance of wild-type Kir2.1 saturated at potentials more hyperpolarized than −100 mV, and that of the D172N mutant showed a slight decrease in the peak conductance. Upon introduction of the S165L mutation, however, neither the wild-type channel nor the D172N mutant reached saturation even at the most hyperpolarized potential recorded (−160 mV) (Fig. 2 C). The same effect was observed in the triple mutant and suggests that the S165L mutation may also affect the permeation properties of the channel.

The Effect of the Amino Acid Residue at Position 165 on Inward Rectification

We next substituted selected amino acids for S165 in the D172N & E224G & E299S triple mutant and analyzed the electrophysiological properties using two-electrode voltage clamp (Fig. 3). The inward rectification properties of the various mutants were classified into two groups: one group with G, I, or L at position 165 showed very weak inward rectification, whereas the other group with E, D, T, or S at position 165 showed relatively strong inward rectification (Figs. 3 and 4 B). In the latter group, the amino acid residue at 165 is hydrophilic and has a $COOH^-$ (E, D) or OH^- group (T, S) in the side

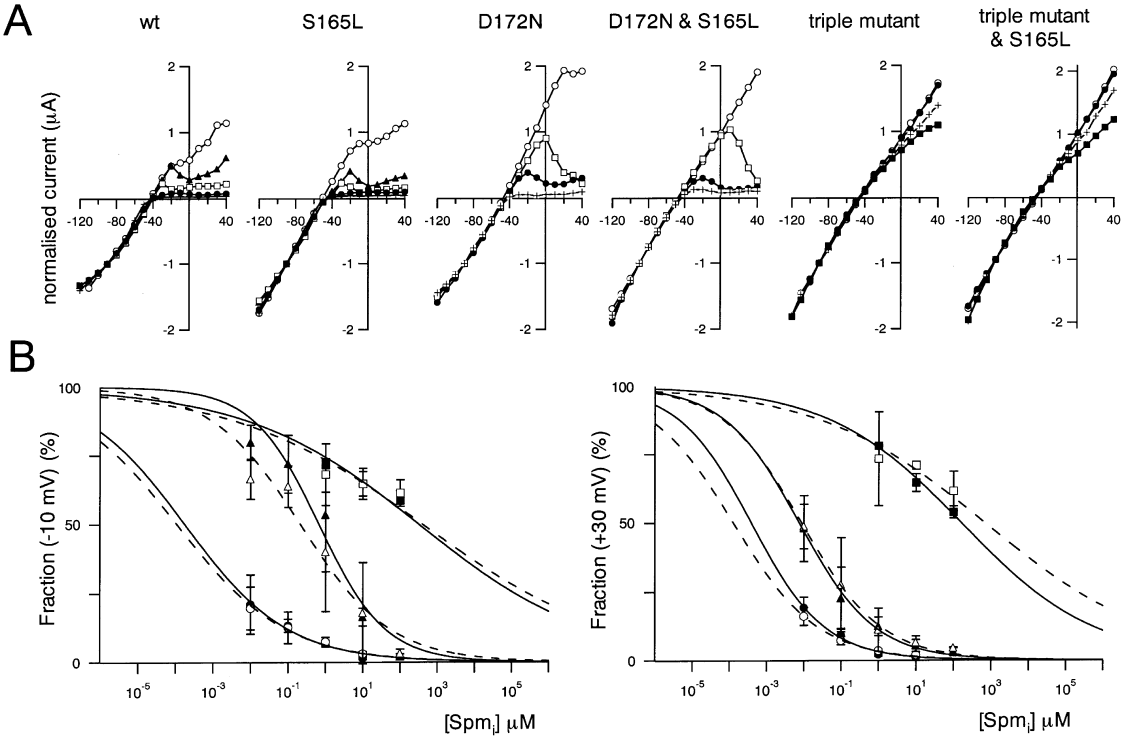

FIGURE 6. Comparison of the susceptibility of macroscopic currents through wild-type and mutant Kir2.1 to blockade by intracellular spermine. (A) Normalized I-V relationships; values were measured 3 s after the onset of each step pulse. Current amplitudes were normalized to the values at −90 mV. The symbols stand for spermine concentrations of 0 μM (○), 0.01 μM (▲), 0.1 μM (□), 1 μM (●) 10 μM (+) and 100 μM (■). (B) Concentration-response relationships for spermine blockade of outward K^+ currents at −10 mV (left) and 30 mV (right). A rectification index was calculated first as the ratio of the current amplitudes at −10 mV or 30 mV to that at −90 mV. A value of 1 was then set as 100% for the data at −10 mV (left), and a value of 2 was set as 100% for the data at +30 mV (right). Symbols depict means ± SD (n = 3–7) for wild-type (●), S165L (○), D172N (▲), D172N & S165L (△), triple mutant (■), and triple mutant & S165L (□) channels. Solid lines (S165) and dotted lines (with S165L mutation) are curves fitted to Hill's equation.

chain. This implies that, as in the cases of D172 (Lu and MacKinnon, 1994) and E224 (Yang et al., 1995) mutants, the electrostatically negative environment of the OH^- group of Ser165 contributes to inward rectification, and that the phenotype of the S165L mutant is not due to the L itself. Still, slight differences were observed even between mutants in the same group (e.g., L and G, D and E) (Fig. 4 B), perhaps due to differences in the size, shape, and chemical properties of the amino acid residue at position165. To further examine the effect of electrostatic charge at this residue, we made an S165K mutant, but it did not allow any detectable current. The analysis summarized below was performed using S165L as a representative mutation.

Comparison of the Susceptibility of Wild-type and Mutant Kir2.1 to Blockade by Spermine

Since inward rectification is caused by blockage of the channel by cytoplasmic Mg^{2+} or polyamines, we next determined how the susceptibility to blockade by these inhibitors was affected by S165L mutation. Macroscopic currents were recorded in the presence of spermine from inside-out membrane patches excised from HEK293T cells expressing wild-type or mutant Kir2.1 (Fig. 5). In the cases shown, prominent outward currents were observed when no spermine was present, indicating that endogenous cytoplasmic polyamines had been washed out. In the case of the D172N mutant, a weak but significant rectification remained consistently, even after intensive exchange of the intracellular solution (Fig. 5–8). We speculate that cytoplasmic blockers tend to remain in D172, but the details are unknown.

The I-V relationships were determined from a set of measurements obtained 3 s after the onset of each step pulse. Because the run-down phenomenon made it very difficult to obtain a full dataset in which the inward current amplitude remained stable throughout, we compared the I-V relationships and rectification using data from multiple patches by normalizing the current amplitude to the values at −90 mV (−40 mV from E_K) (Fig. 6 A). In addition, because blockage by spermine showed a strong voltage dependency, especially in the D172N and D172N & S165L mutants, rectification indexes at two voltages, −10 mV (40 mV from E_K) and 30 mV (80 mV from E_K) were calculated.

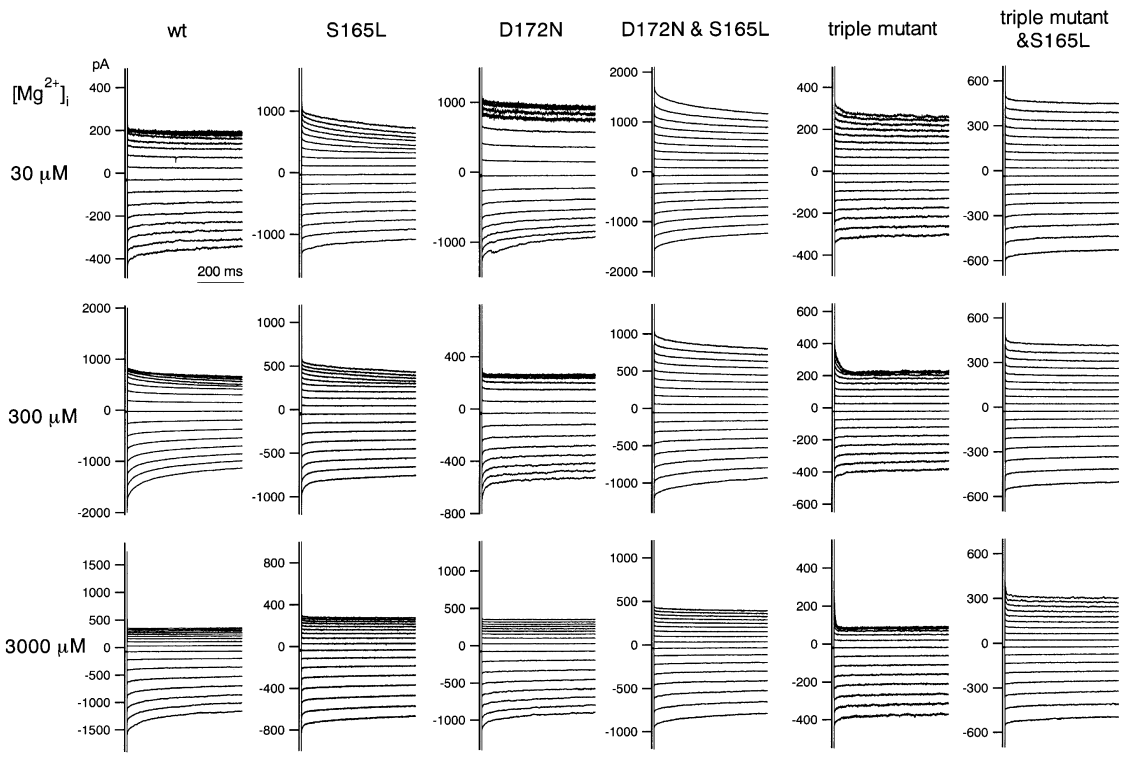

FIGURE 7. Macroscopic currents recorded in the presence of the indicated concentrations of intracellular Mg^{2+} from excised patches of HEK293T cells expressing wild-type and mutant Kir2.1. The concentrations of $Mg^{2+}{}_i$ are shown on the left. $K^+{}_o$ in the pipette was 20 mM, and $K^+{}_i$ in the bath was 140 mM. The calculated E_K was −49 mV. The holding potential was −50 mV, and step pulses from 40 to −120 mV were applied in 10-mV decrements.

An index of 2 was set as 100% at 30 mV because the driving force at that voltage was twice that at −90 mV when E_K is −50 mV; an index of 1 was set as 100% at −10 mV because the driving force at that voltage was the same as at −90 mV. The means ± SD (n = 3–7) of the fractions were then plotted against spermine concentration (Fig. 6 B). The fractions at −10 and 30 mV in e.g., 1 μM spermine did not change by introducing S165L mutation significantly ($P > 0.05$, Student's unpaired t test) on the backgrounds of wild-type, D172N and the triple mutant.

The plotted mean values were then fitted with Hill's equation (Fig. 6 B). Ki and Hill coefficient values obtained from the fitting at −10 mV were: 0.00018 μM and 0.32 (wild-type), 0.00011 μM and 0.30 (S165L), 0.67 μM and 0.49 (D172N), 0.21 μM and 0.36 (D172N & S165L), 320 μM and 0.19 (triple mutant), 400 μM and 0.17 (triple mutant & S165L). The values at 30 mV were: 0.00039 μM and 0.44 (wild-type), 0.00013 μM and 0.38 (S165L), 0.0075 μM and 0.43 (D172N), 0.0087 μM and 0.40 (D172N & S165L), 160 μM and 0.24 (triple mutant), 680 μM and 0.19 (triple mutant & S165L).

The wild-type Kir 2.1 channel was highly sensitive to spermine; D172N was less so, and D172N & E224G & E299S was even less sensitive than D172N. As indicated by the overlap of the fitted curves depicted by the solid (Ser165) and dotted (S165L mutation) lines in Fig. 6 B, S165L mutation did not clearly affect the susceptibility to spermine blockade. Apparently, D172, E224, and E299 are critical for Kir2.1 sensitivity to spermine, but S165 is not. This confirms the assumption that spermine plugs the pore at the level of D172 and suggests that S165, which is situated at a narrow site farther from the intracellular side of the membrane than D172, is not accessible to bulky cytoplasmic spermine.

Comparison of the Susceptibility of Wild-type and Mutant Kir2.1 to Blockade by $Mg^{2+}{}_i$

Addition of free $Mg^{2+}{}_i$ (calculated as described in MATERIALS AND METHODS) blocked the outward current through the wild-type Kir2.1 at depolarized potentials almost instantaneously, but the effect developed much more slowly in the S165L mutant (Fig. 7). This slow blockade of outward currents was characteristic of S165L mutation, and was also observed in the D172N & S165L double mutant and in the triple & S165L mutant. In addition, it was clear from the normalized I-V relationship to the value at −90 mV (−40 mV from E_K) that the strength of the rectification at each $Mg^{2+}{}_i$

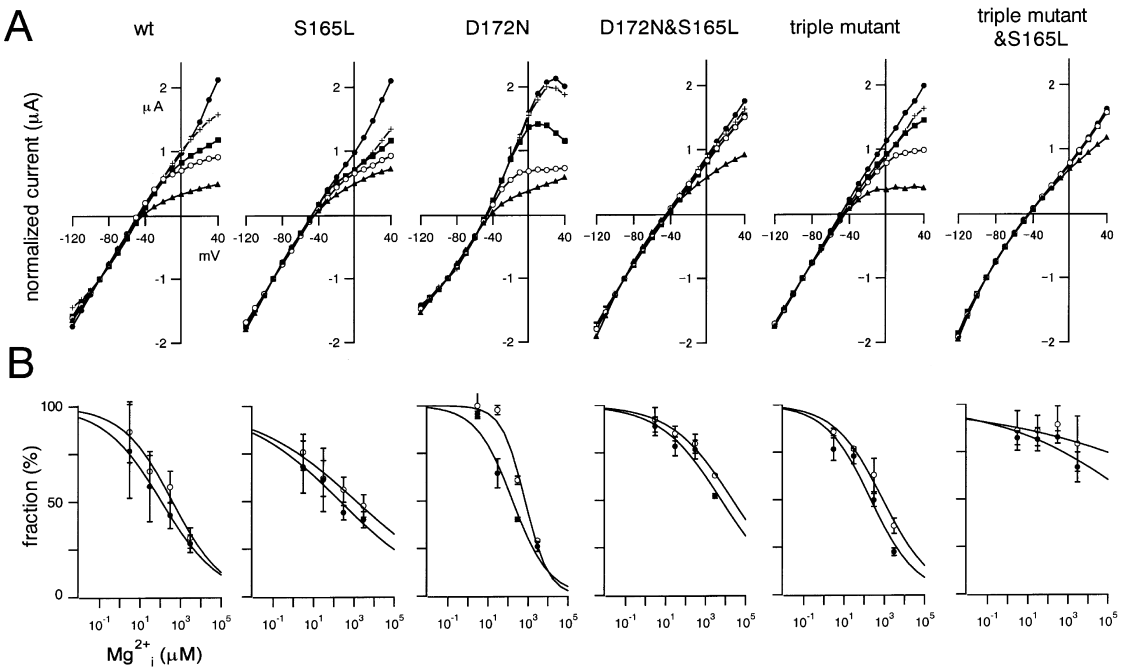

FIGURE 8. Comparison of the susceptibility of macroscopic currents through wild-type and mutant Kir2.1 to blockade by intracellular Mg^{2+}. (A) Normalized I-V relationships. Values were measured 500 ms after the onset of each step pulse. The symbols stand for Mg^{2+} concentrations of: 0 μM (●), 3 μM (+), 30 μM (■), 300 μM (○), and 3,000 μM (▲). The current amplitudes were normalized to the values at −90 mV. (B) Dose–response relationships for Mg^{2+}_i blockade of outward K^+ currents at −10 mV (○) and at 30 mV (●). The rectification index was calculated first as the ratio of the current amplitudes at −10 or 30 mV to that at −90 mV. A value of 1 was set as 100% for the data at −10 mV, and a value of 2 was set for the data at 30 mV. Symbols depict means ± SD (n = 3–7). To improve the fitting, the rectification index of 1.75 at 30 mV was set as 100% in the case of the D172N mutant, and 2.25 was set as 100% in the case of the triple & S165L mutant. This is thought to be because of changes in rectification properties in the absence of blockers.

concentration—i.e., the susceptibility to blockade by Mg^{2+}_i—was reduced by the introduction of the S165L mutation in all cases (Fig. 8 A). Mg^{2+}_i concentration-block relationships were determined by normalizing the current amplitude at 30 mV (●) and −10 mV (○) to the values at −90 mV. In most cases, rectification indexes of 2 and 1 were set as 100% at 30 and −10 mV, respectively. For the data from the D172N and triple & S165L mutants, indexes of 2.25 and 1.75 were set as 100% at 30 mV. These adjustments were done to practically optimize the curve fitting and we speculate that they reflect changes in the rectification properties in the absence of cytoplasmic blockers of these two channels. The fractions at −10 and 30 mV in, for example, 3,000 μM Mg^{2+} changed by introducing S165L mutation significantly ($P < 0.01$, Student's unpaired t test) on the backgrounds of wild-type, D172N, and triple mutant.

The plotted mean values were then fitted with Hill's equation (Fig. 8 B). The Ki and Hill coefficient values at −10 mV were: 410 μM and 0.35 (wild-type), 1310 μM and 0.17 (S165L), 740 μM and 0.77 (D172N), 23000 μM and 0.28 (D172N & S165L), 830 μM and 0.39 (triple mutant), 9.9×10^8 μM and 0.11 (triple mutant & S165L). The values at 30 mV were: 120 μM and 0.30 (wild-type), 210 μM and 0.18 (S165L), 190 μM and 0.47 (D172N), 6,100 μM and 0.28 (D172N & S165L), 210 μM and 0.38 (triple mutant), 2.5×10^6 μM and 0.13 (triple mutant & S165L).

These results suggest that either S165 or D172 alone could account for the channel's sensitivity to Mg^{2+}_i and that mutations of both sites dramatically diminished sensitivity. Together, these findings indicate that both D172 and S165 play a crucial role in determining the susceptibility of Kir2.1 to blockade by Mg^{2+}_i. We therefore conclude that S165 is a novel residue crucially involved in Mg^{2+}_i blockade.

Effect of S165L Mutation on Rb^+ Permeation of Kir 2.1

Macroscopic currents in 10 mM K^+ (Fig. 9 A) and 10 mM Rb^+ (Fig. 9 B) were recorded from the same oocytes using two-electrode voltage clamp; the I-V relationships are plotted in Fig. 9 C. Rb^+ permeance indexes (Thompson et al., 2000), calculated as $I_{Rb+}(-120\ mV)/I_{K+}(-120\ mV)$, are shown in Fig. 11 A. Wild-type Kir 2.1 showed a very low Rb^+ permeance, and S165L mutation increased it dramatically. D172N mutation caused only a slight increase. In the background of

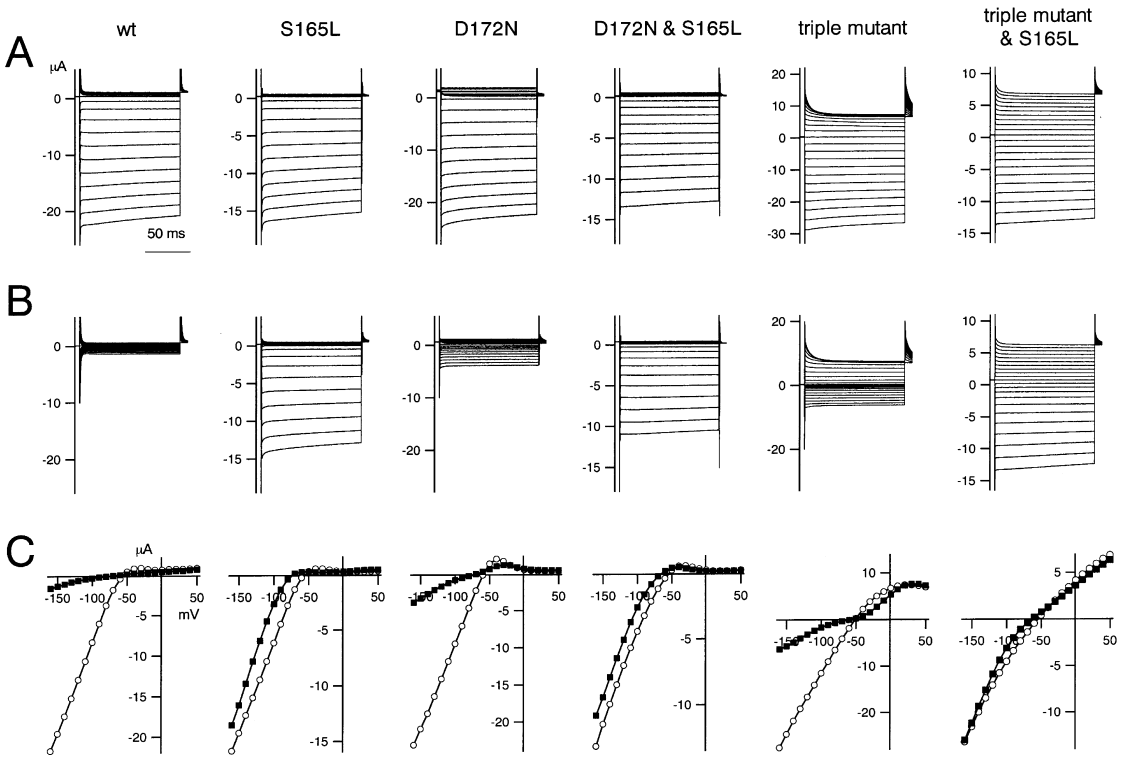

FIGURE 9. Comparison of macroscopic K^+ and Rb^+ currents through wild-type and mutant Kir2.1. (A and B) Currents recorded using two-electrode voltage clamp with *Xenopus* oocytes expressing wild-type and mutant Kir2.1 in the presence of either 10 mM K^+ and 80 mM NMG (A) or 10 mM Rb^+ and 80 mM NMG (B). The holding potential was −50 mV, and step pulses from 50 to −160 mV were applied in 10-mV decrements. (C) I-V relationships determined from the data in (A) and (B); values are current amplitudes measured 50 ms after the onset of each step pulse in 10 mM K^+ (○) and 10 mM Rb^+ (■).

D172N and the triple mutant, S165L mutation again increased Rb^+ permeance dramatically (Fig. 11 A).

Next we aimed to analyze the permeability ratios of K^+ and Rb^+ by measuring the reversal potentials in K^+_o and in Rb^+_o solution. Xie et al. (2002) reported that the surface charge screening component by polyamine affects the apparent reversal potential by shifting it toward negative direction from the real value. The very small amplitude of outward current in the presence of polyamine also makes the determination of reversal potentials inaccurate. For these two reasons, we measured the reversal potentials by inside-out patch clamp recording in the absence of intracellular Mg^{2+}_i and spermine. Macroscopic currents were recorded by applying ramp pulses of 800 ms from −150 to 50 mV, in 20 mM $[K_o^+]$/140 mM $[K_i^+]$ (Fig. 10 A) and 20 mM $[Rb_o^+]$/140 mM $[K_i^+]$ (Fig. 10 B). $E_{rev(K+o)}$ and $E_{rev(Rb+o)}$ of wild-type Kir2.1 were −49.8 ± 1.80 mV and −69.6 ± 4.0 mV (Fig. 11 B). In comparison with the wild-type, $E_{rev(Rb+o)}$ were shifted to depolarized potentials while $E_{rev\ (K+o)}$ did not change in the S165L, D172N, and D172N & S165L mutants. The values were −48.9 ± 1.6 mV ($E_{rev(K+o)}$) and −61.7 ± 3.4 mV ($E_{rev(Rb+o)}$) in the S165L mutant, −48.4 ± 1.7 mV ($E_{rev(K+o)}$) and −61.3 ± 2.5 mV ($E_{rev(K+o)}$) in the D172N mutant, −50.0 ±1.6 mV ($E_{rev(K+o)}$) and −60.3 ± 1.5 mV ($E_{rev(Rb+o)}$) in the D172N & S165L mutant (Fig. 11 B). The permeability ratios of Rb^+ and K^+ (P_{Rb+}/P_{K+}), calculated from the shift of the reversal potential by the Nernst equation, were 0.46 (wt), 0.60 (S165L), 0.60 (D172N), and 0.66 (D172N & S165L), showing that both S165L and D172N mutation equally increased permeability of Rb^+ relative to K^+.

Together, S165 and D172, which determine the susceptibility to intracellular blockers, were shown to be crucial determinants of Rb^+ permeability. That D172N mutation caused only a slight increase in Rb^+ permeance, but S165L mutation dramatically increased it is indicative of the difference in the functions D172 and S165 for Rb^+ permeation.

Comparison of the Single-channel Conductances through Wild-type and Mutant Kir2.1

Single-channel recordings were obtained from *Xenopus* oocytes using the cell-attached patch configuration in 140 mM K^+_o. Recordings at −80, −120, and −160 mV are shown in Fig. 12, although in the case of the D172N & S165L double mutant, data were recorded at −120,

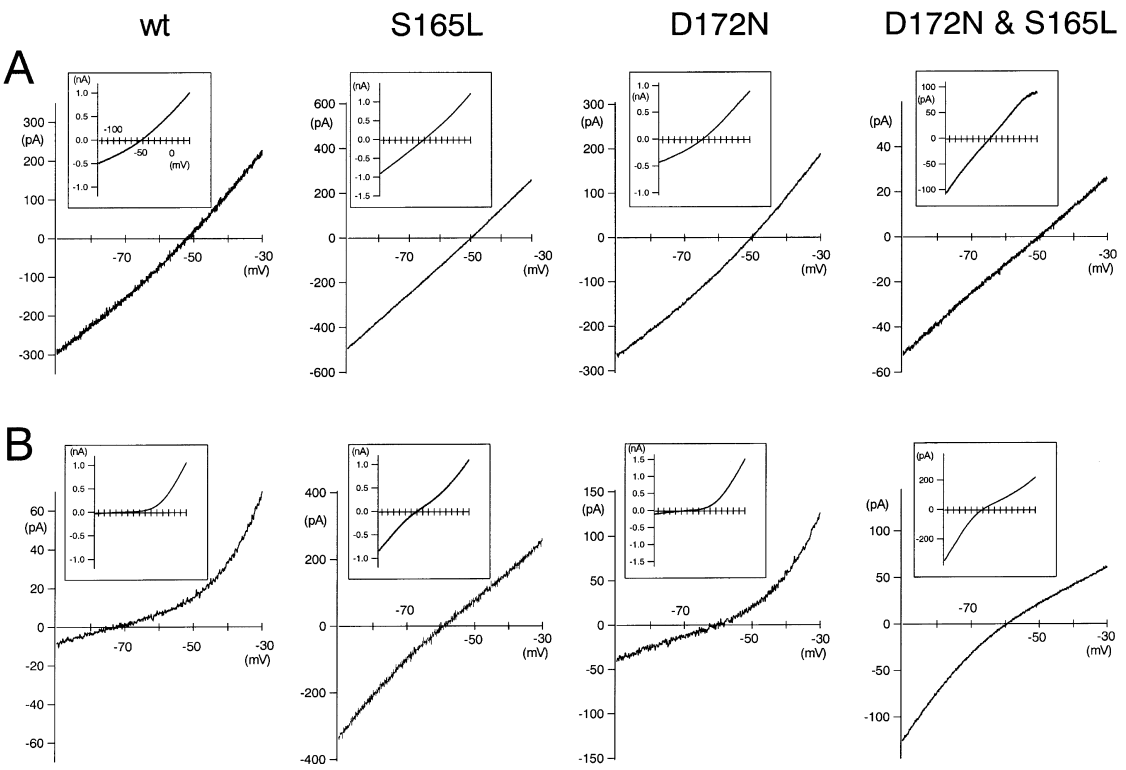

FIGURE 10. Comparison of $E_{rev\ (K+o)}$ and $E_{rev\ (Rb+o)}$ between wild-type and mutant Kir2.1. (A and B) Macroscopic current recordings under inside-out patch clamp from HEK293T cells expressing wild-type Kir2.1 or the mutants in the absence of $Mg^{2+}{}_i$ and spermine. The extracellular solutions contained 20 mM K^+ (A) or 20 mM Rb^+ (B). The holding potential was −50 mV, and ramp pulses from −150 to 50 mV for 800 ms were applied. Recordings from −130 to 30 mV were shown in the insets, and the ranges between −90 and −30 mV were enlarged to demonstrate the reversal potentials clearly.

−160, and −200 mV because the single channel current amplitudes were very small. The I-V relationships and the accumulated data on the single-channel conductance shown in Fig. 12, B and C, respectively, suggest that S165 contributes to the permeation properties in cooperation with D172.

Accessibility of the S165C Residue by Cys-modifying Reagents Applied from either the Intracellular or Extracellular Side

To gain insight of the structure of S165 and surrounding regions of Kir2.1, we next analyzed the accessibility of S165C residue by Cys-reacting reagents from either extracellular (Fig. 13, A and C) or intracellular (Fig. 13, B and D) side.

The accessibility from the extracellular side was examined as we described previously (Kubo et al., 1998). As endogenous Cys149 of the wild-type Kir2.1 gives a background modification, we first introduced C149F mutation, and used it as a negative control. We then introduced F147C mutation at the external entrance of the pore on the background of C149F, and used this C149F & F147C mutant as a positive control of modification. S165L mutation was introduced also on the background of C149F (C149F & S165L). Application of MTSET (100 μM), MTSEA (100 μM), or Cd^{2+} (100 μM) decreased the current of C149F & F147C, but not of C149F or of C149F & S165C, showing the lack of accessibility of S165C by these reagents from extracellular side (Fig. 13, A and C). As we observed that T141C is accessible from extracellular side (Kubo et al., 1998), S165 was shown to locate at a deeper position from extracellular side than T141.

Lu et al. (1999) reported a systematic analysis of the accessibility of various amino acid residues of Kir2.1 from intracellular side. They first made a construct named IRK1J as a negative control in which endogenous Cys residues causative of modification from inside were mutated. They showed that S165C could not be modified from intracellular side by MTSET or MTSEA. To confirm their observation, we performed a similar analysis using IRK1J as a negative control and IRK1J & S165C. We observed that neither MTSET (2 mM) nor MTSEA (2.5 mM) caused clear modification of IRK1J & S165L at a level apparently different from that observed in IRK1J (Fig. 13, B and D), suggesting that S165C was not accessible from intracellular side by these reagents. We also tried to analyze the effect of Cd^{2+}, but failed to draw a reliable conclusion, due to a severe reversible block of current which hindered an accurate estimation of the extent of Cys modification.

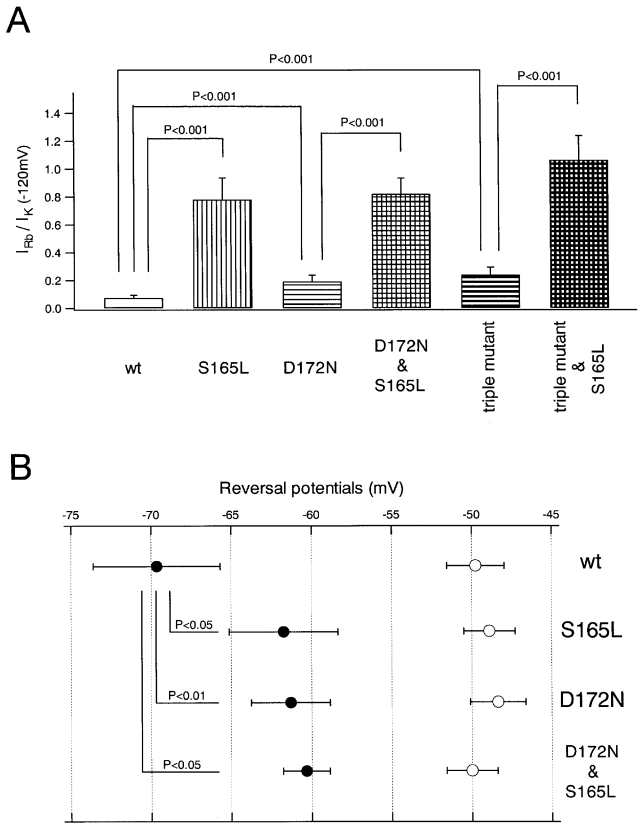

FIGURE 11. Quantitative comparison of Rb^+ permeance and the permeability ratio of Rb^+ and K^+ of wild-type Kir2.1 and the mutants. (A) The Rb^+/K^+ ratios of current amplitudes at −120 mV were calculated from the data in Fig. 9 C; means ± SD (n = 7–12 of each group) and values of P (Student's unpaired t tests) are shown. (B) Means and SD (n = 3–5 of each group) of reversal potentials shown in Fig. 10. The open and filled symbols show values of $E_{rev(K+o)}$ and $E_{rev(Rb+o)}$, respectively. The P values (Student's unpaired t tests) are also indicated.

Significance of the Corresponding Amino Acid Residue to Ser 165 in other Kir Family Members

To examine whether the amino acid residue corresponding to S165 of Kir 2.1 is important for inward rectification of currents through other Kir family members, we substituted S164 in Kir 1.1 and L169 in sWIRK. The Kir1.1 S164L mutant did not allow any detectable current. In the case of sWIRK, we substituted L169 with S, T, Y, E, D, Q, N, C, G, A, V, I, or K, but only the L169I mutant allowed detectable current that was very similar to that of the wild-type sWIRK (unpublished data).

DISCUSSION

In this study we introduced various point mutations selected on the basis of a sequence comparison of Kir2.1 and sWIRK into wild-type Kir2.1 and its D172N and D172N & E224G & E299S mutants. Our aim was to identify one or more structural determinants of inward rectification. We succeeded in identifying S165 as one such site based on the following comparisons between wild-type and mutant Kir2.1 channels. (a) Both the S165L and D172N mutants showed diminished susceptibility to blockade by Mg^{2+}_i, and the susceptibility was further reduced in the D172N & S165L double mutant (Figs. 7 and 8). (b) D172N but not S165L mutation reduced the susceptibility to spermine blockade. That the susceptibility to spermine was reduced still further in the D172N & E224G & E299S triple mutant than in the D172N mutant is indicative of the importance of E224 and E299 for the susceptibility to spermine (Figs. 5 and 6). (c) Rb^+ permeance—i.e., the amplitude of the Rb^+ inward current—was increased slightly in the D172N mutant and much more dramatically in the S165L mutant in comparison with the wild-type. P_{Rb+}/P_{K+} of D172N and S165L mutant were equally higher than the wild-type (Figs. 9–11). (d) Whereas the single-channel conductance of the S165L mutant was reduced significantly, the change was not clear in the D172N mutant (Fig. 12). (e) We also observed that a S165C mutant on the back ground in which endogenous Cys residues were substituted could not be modified by Cys-reacting reagents from either the intracellular or extracellular side (Fig. 13).

Functional Roles of the Four Residues that Define the Inward Rectification Properties of Kir2.1

The scheme shown in Fig. 14 depicts the four amino acid residues identified to be critical for inward rectification of currents through Kir2.1 (D172, E224, E299, and S165).

(a) D172. This residue was identified in 1994 as a site that determines the sensitivity to Mg^{2+}_i and affects the activation phase upon hyperpolarization (Lu and MacKinnon, 1994; Stanfield et al., 1994; Wible et al., 1994). It was later shown to also be critical for the susceptibility to blockade by polyamines (Yang et al., 1995). It has been speculated that spermine plugs the pore at D172 (Lopatin et al., 1995; Pearson and Nichols, 1998) and that partial blockade by Mg^{2+}_i occurs at this site (Oishi et al., 1998).

(b and c) E224 and E299. E224, which was originally thought to be situated in the cytoplasmic region after M2 (Kubo et al., 1993a), was shown in 1995 to contribute to the susceptibility to the blockade by polyamines and to form part of the permeation pathway (Yang et al., 1995). In addition, it was reported recently that E299, which was originally thought to be near the midpoint of the long-cytoplasmic chain after M2 (Kubo et al., 1993a) also contributes to inward rectification and, like E224, forms part of the inner pore (Kubo and Murata, 2001; Xie et al., 2002). In that study, we considered the likelihood that E224 and

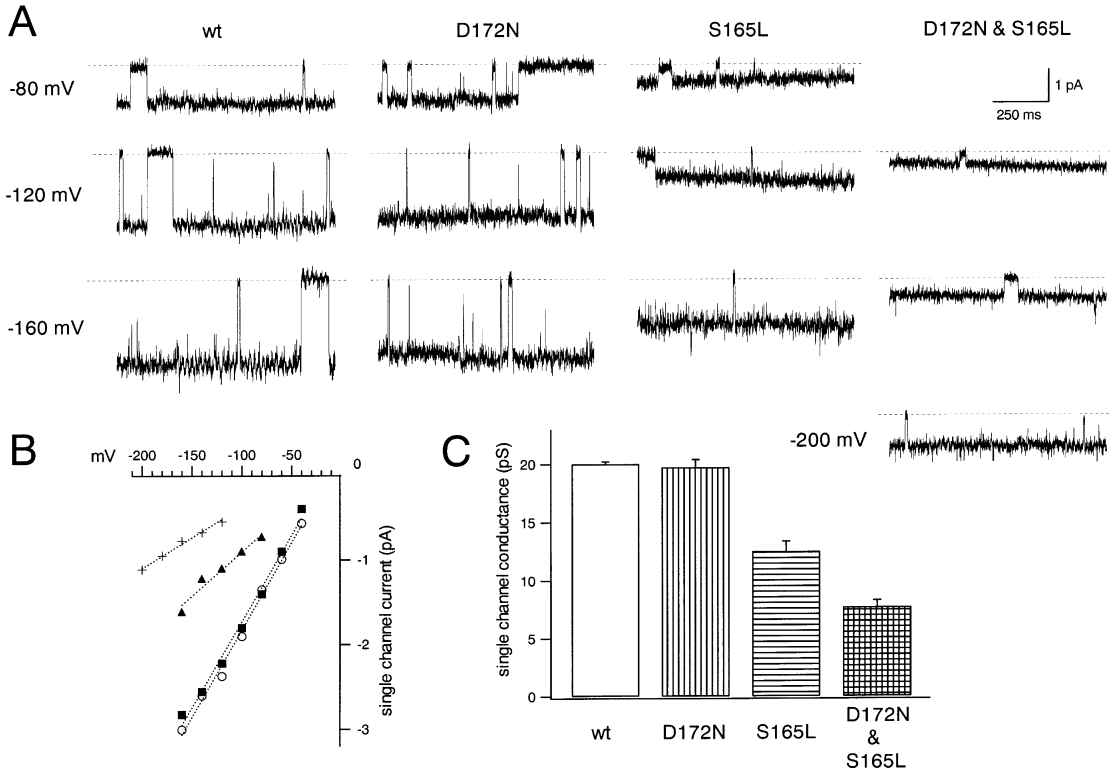

FIGURE 12. Comparison of single-channel currents through the wild-type Kir2.1 and the mutants. (A) Representative single-channel currents recorded from *Xenopus* oocytes using the cell-attached patch configuration. The K^+_o in the pipette and in the bath were 140 mM. The holding potential for the displayed recordings were −80, −120, and −160 mV for the wild-type, D172N, and S165L channels, and were −120, −160, and −200 mV for the D172N & S165L double mutant. The dashed lines indicate the zero current level after subtracting the leak current. (B) Relationship of single-channel current amplitude and holding potential for wild-type (○), D172N (■), S165L (▲), and D172N & S165L (+) channels. (C) Single-channel conductance calculated from the slopes of the plots in B; plotted are means ± SD (n = 4–6).

E299 are located at the inner vestibule and serve as intermediate binding (nonplugging) sites that facilitate entry and exit of spermine to and from the final pore-plugging binding site located deeper in the pore (Kubo and Murata, 2001). It was postulated that E224 and E299 serve to increase the local concentration of spermine at the inner vestibule (Kubo and Murata, 2001; Xie et al., 2002).

(d) S165. In the present work, we identified S165 as the fourth site that contributes to the inward rectification of currents through Kir 2.1. S165L mutation affected the susceptibility to blockade by Mg^{2+}_i, but not by spermine (Figs. 2–8).

Structure of the Kir 2.1 Inner Pore with Respect to the Susceptibility to Intracellular Blockers

The high-resolution structure of the bacterial KcsA channel was resolved by X-ray crystallography (Doyle et al., 1998) and might be applicable to the structure of all K^+ channels. If this is the case, S165 of Kir 2.1 corresponding to M96 of KcsA would be predicted to form an intersubunit hydrogen bond and not to face to the aqueous pore. Our observation that S165C was not modified by Cys-reacting regents (Fig. 13) could be explained by this structure. Also, as S165L mutation might produce severe changes in the overall structure of the pore by destroying the hydrogen bonds, the significant change in Rb^+ permeance we observed could be explained by this assumption (Figs. 9–11). However, by making several different substitutions at S165 on the background of the D172N & E224G & E299Q mutant, we observed that functional channel property was maintained, and that the negatively charged atmosphere of the side chain determines the inward rectification property (Figs. 3 and 4). These results imply that S165 faces to the aqueous pore rather than that it forms an intersubunit hydrogen bond.

Based on random mutagenesis and a yeast genetic screening method, Minor et al. (1999) concluded that the structural correspondence between Kir 2.1 and KcsA is not necessarily high. Their identification of the pore-lining and M1/M2 intersubunit interface residues of Kir2.1 indicated that the M2 region of Kir 2.1 forms an α-helix and S165, C169, D172, and I176 are not part of an intersubunit interface, but are surface residues

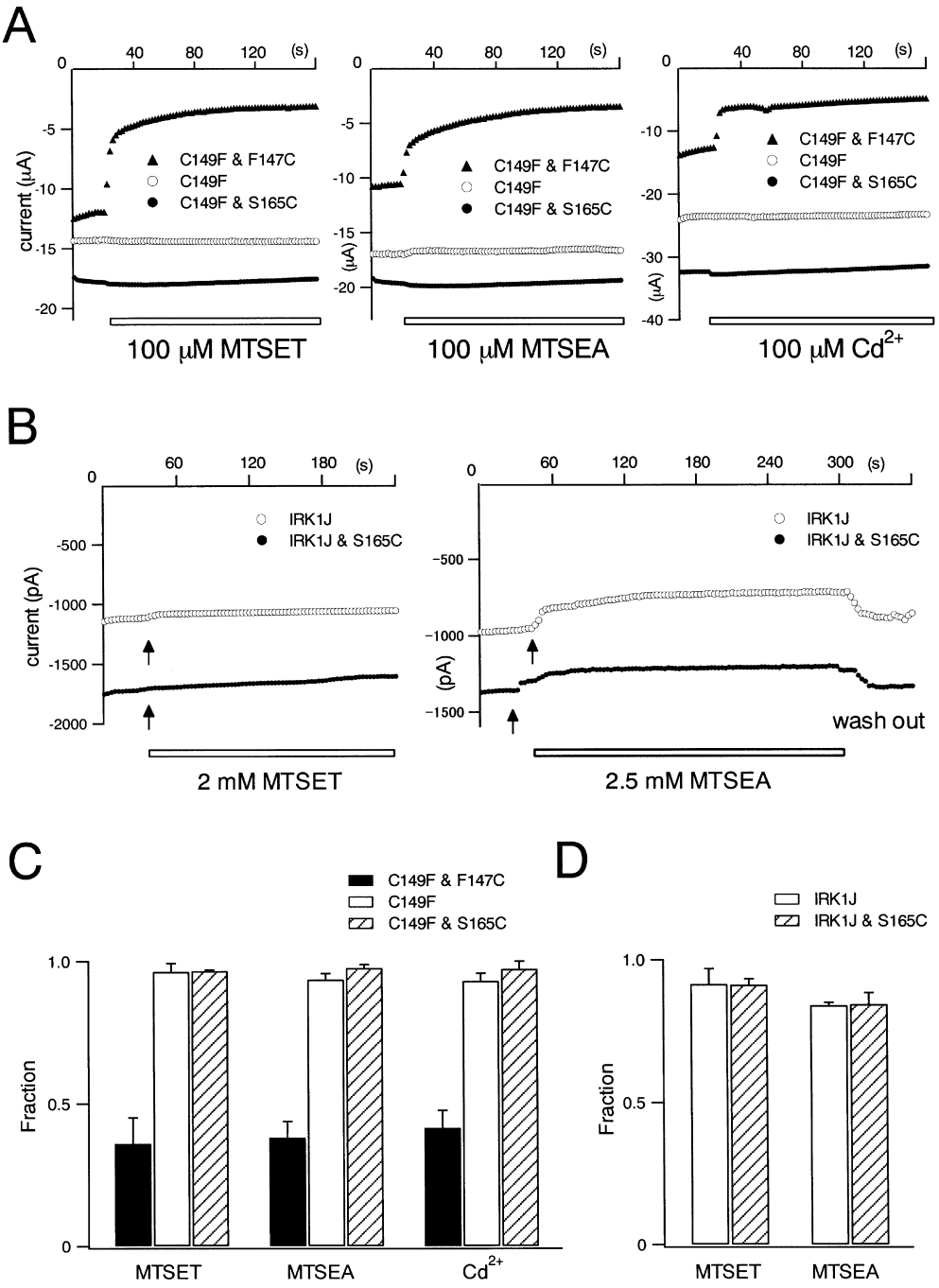

FIGURE 13. Accessibility of S165C by cys-modifying reagents from extracellular and intracellular sides. (A) Currents recorded under two-electrode voltage clamp from *Xenopus* oocytes. The effects of either 100 μM MTSET, 100 μM MTSEA, or 100 μM Cd^{2+} were shown. The symbols are (○), C149F (negative control); (▲), C149F & F147C (positive control); and (●), C149F & S165C. Test pulses for 100 ms were given every 2 s to −130 mV from a holding potential of −30 mV, and current amplitudes were measured at 50 ms from the onset of each test pulse. (B) Currents recorded from transfected HEK293T cells under inside-out patch clamp. The effects of 2 mM MTSET or 2.5 mM MTSEA were analyzed. Test pulses for 200 ms were given every 3 s to −120 mV from a holding potential of −50 mV, and current amplitudes were measured at 100 ms from the onset of each test pulse. (C and D) Fractions of the residual current amplitudes after application of cys-modifying reagents from extracellular side at 120 s (C) and from intracellular side at 180 s (D). The values of means ± SD (n = 4) are shown.

mediating protein–water interaction (Minor et al., 1999). This proposal is consistent with our observation that various mutations at S165 determine the susceptibility to blockade by Mg^{2+}_i.

By combining cysteine scanning mutagenesis and covalent chemical modification, Lu et al. (1999) determined that the inner vestibule of Kir 2.1 at the level of D172 is spacious enough to fit multiple methane-thio-sulfonate reagents (e.g., MTSET and MTSEA). They also reported that these reagents did not modify S165. We repeated this experiment using MESET and MESEA and confirmed that S165C is not covalently modified. We interpret these data to imply most likely that the inner pore at the level of S165 is too narrow for methane-thio-sulfonate reagents to access, although S165 faces to the aqueous pore. Our finding that the S165L mutant did not change the susceptibility to spermine blockade, but decreased the susceptibility to Mg^{2+}_i blockade, goes very well with this interpretation. Minor et al. (1999) reported that S165 is situated two α-helix turns up from D172. In that context, our findings suggest that the inner vestibule of Kir2.1 is rela-

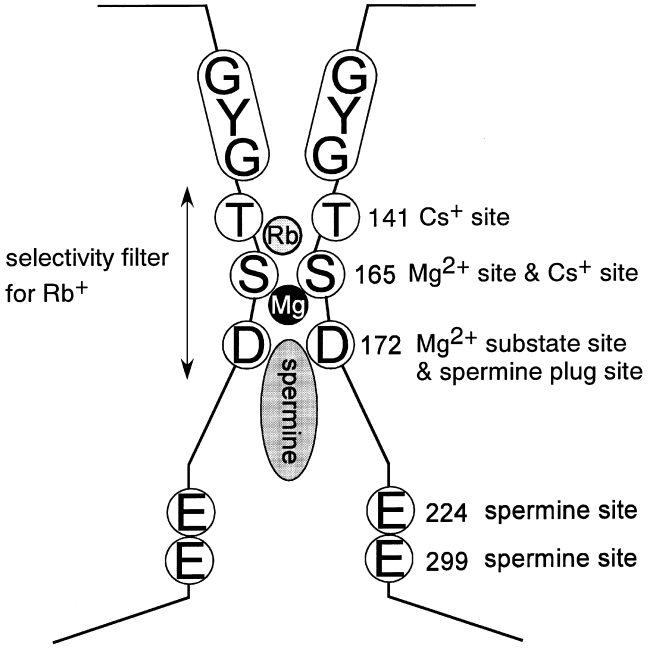

FIGURE 14. Model of the pore structure of Kir2.1. The scheme explains the location and functional role of T141, S165, D172, E224, and E299.

tively wide at the level of D172, but has narrowed at the level of S165; consequently, $Mg^{2+}{}_i$ but not spermine can access S165 (Fig. 14).

As mutants of other Kir family members at the corresponding amino acid to S165, S164L of Kir1.1 and L169S of sWIRK, did not allow any detectable current, it is likely that the structures of Kir1.1, sWIRK and Kir 2.1 differ significantly—e.g., Kir 1.1 S164 and sWIRK L169 might participate in inter-subunit hydrogen bonding, as is known for KcsA.

S165 Is the Key Residue Accessed by Both Extracellular and Intracellular Blockers

Thompson et al. (2000) reported that the S165L mutant showed large inward Rb^+ currents at negative voltages below the reversal potential, although inward currents through wild-type Kir 2.1 were blocked by extracellular Rb^+; that Rb^+ permeance was increased further in the S165L & T141A double mutant, and even further in the S165L & T141A & D172N triple mutant; that both S165L and T141A mutation significantly reduced Cs^+ blockade; that the S165L and T141A double mutant were nearly insensitive to Cs^+; and that D172N mutation did not alter Cs^+ sensitivity. Since S165 is situated farther from the extracellular side than the GYG K^+ selectivity filter (Heginbotham et al., 1992; Doyle et al., 1998; Minor et al., 1999), they speculated that extracellular blocking cations, such as Rb^+ and Cs^+, must traverse the GYG selectivity filter in Kir 2.1.

In the present study we analyzed the effect of S165L mutation on Rb^+ permeance and P_{Rb+}/P_{K+} in wild-type Kir 2.1 and the D172N mutant. Rb^+ permeability was increased by D172N and S165L mutation, and inward Rb^+ currents were dramatically increased by S165L mutation, but only slightly by D172N mutation. This suggests that both S165 and D172 play a role in Rb^+ permeation and selectivity (Fig. 14), and their functions differ.

T141 is known to be easily accessible to several cations from the extracellular side. For instance, we used a cysteine scan mutagenesis analysis of a T141C mutant to show that Cd^{2+} could access the site from the extracellular side (Kubo et al., 1998). In addition, Dart et al. (1998) reported accessibility of Ag^+ to this site, and Alagem et al. (2001) showed that T141 is involved in the stabilization of Ba^{2+} binding. When we examined the accessibility of S165C to Cd^{2+} from extracellular side, we observed no modification. S165 is thus apparently located at a position farther from extracellular side than T141, at a point where the pore is narrower and accessible to Rb^+ and Cs^+, but not to Cd^{2+} (Fig. 14). We therefore propose that Ser165 forms the narrowest part of the pore, the point at which both extracellular and intracellular blockers plug the permeation pathway. This makes S165 a key determinant of ion permeability, selectivity and rectification.

We are grateful to Drs. J. Yang (Columbia University), C.G. Nichols (Washington University), and J. Miyazaki (Osaka University) for providing us with IRK1J cDNA, Kir 1.1 cDNA, and $pCXN_2$ expression vector, respectively. We would like to thank Dr. K. Ishihara (Saga Medical School) for advice and suggestions; Drs. T. Misaka, (Tokyo Medical and Dental University), H. Abe (Tokyo Medical and Dental University), Y. Murata (Okazaki National Research Institute), K. Nakajo (Tokyo Medical and Dental University), H. Matsuda (Kansai Medical School), N. Ogata (Hiroshima University), and K. Takahashi (Meiji University of Pharmacy) for discussion; and Ms. R. Watanabe for technical assistance. We also appreciate invaluable advice of the reviewers.

This work was supported partly by the research grants from the Ministry of Education, Science, Sports, Culture, and Technology of Japan and from foundations of Umami, Kowa, Novartis, and Salt Science.

Submitted: 9 July 2002
Revised: 25 September 2002
Accepted: 26 September 2002

REFERENCES

Alagem, N., M. Dvir, and E. Reuveny. 2001. Mechanism of Ba^{2+} block of a mouse inwardly rectifying K1 channel: differential contribution by discrete residues. *J. Physiol.* 534:381–393.

Bond, C.T., M. Pessia, X.M. Xia, A. Lagrutta, M.P. Kavanaugh, and J.P. Adelman. 1994. Cloning and expression of a family of inward rectifier potassium channels. *Receptors Channels.* 2:183–191.

Dart, C., M.L. Leyland, P.J. Spencer, P.R. Stanfield, M.J. Sutcliffe. 1998. The selectivity filter of a potassium channel, murine Kir2.1, investigated using scanning cysteine mutagenesis. *J. Physiol.* 511: 25–32.

Doyle, D.A., J. Morais Cabral, R.A. Pfuetzner, A. Kuo, J.M. Gulbis,

S.L. Cohen, B.T. Chait, and R. MacKinnon. 1998. The structure of the potassium channel: molecular basis of K^+ conduction and selectivity. *Science.* 280:69–77.

Fakler, B., U. Brandle, E. Glowatzki, S. Weidemann, H.P. Zenner, and J.P. Ruppersberg. 1995. Strong voltage-dependent inward rectification of inward rectifier K^+ channels is caused by intracellular spermine. *Cell.* 80:149–154.

Ficker, E., M. Taglialatela, B.A. Wible, C.M. Henley, and A.M. Brown. 1994. Spermine and spermidine as gating molecules for inward rectifier K^+ channels. *Science.* 266:1068–1072.

Guo, D., and Z. Lu. 2000. Pore block versus intrinsic gating in the mechanism of inward rectification in strongly rectifying IRK1 channels. *J. Gen. Physiol.* 116:561–568.

Heginbotham, L., T. Abramson, and R. MacKinnon. 1992. A functional connection between the pores of distantly related ion channels as revealed by mutant K^+ channels. *Science.* 258:1152–1155.

Ho, K., C.G. Nichols, W.J. Lederer, J. Lytton, P.M. Vassilev, M.V. Kanazirska, and S.C. Hebert. 1993. Cloning and expression of an inwardly rectifying ATP-regulated potassium channel. *Nature.* 362:31–38.

Inagaki, N., T. Gonoi, J.P.T. Clement, N. Namba, J. Inazawa, G. Gonzalez, L. Aguilar-Bryan, S. Seino, and J. Bryan. 1995a. Reconstitution of IKATP: an inward rectifier subunit plus the sulfonylurea receptor. *Science.* 270:1166–1170.

Inagaki, N., Y. Tsuura, N. Namba, K. Masuda, T. Gonoi, M. Horie, Y. Seino, M. Mizuta, and S. Seino. 1995b. Cloning and functional characterization of a novel ATP-sensitive potassium channel ubiquitously expressed in rat tissues, including pancreatic islets, pituitary, skeletal muscle, and heart. *J. Biol. Chem.* 270:5691–5694.

Ishihara, K., M. Hiraoka, and R. Ochi. 1996. The tetravalent organic cation spermine causes the gating of the IRK1 channel expressed in murine fibroblast cells. *J. Physiol.* 491:367–381.

Koyama, H., K. Morishige, N. Takahashi, J.S. Zanelli, D.N. Fass, and Y. Kurachi. 1994. Molecular cloning, functional expression and localization of a novel inward rectifier potassium channel in the rat brain. *FEBS Lett.* 341:303–307.

Kubo, Y., T.J. Baldwin, Y.N. Jan, and L.Y. Jan. 1993a. Primary structure and functional expression of a mouse inward rectifier potassium channel. *Nature.* 362:127–133.

Kubo, Y., T. Miyashita, and K. Kubokawa. 1996. A weakly inward rectifying potassium channel of the salmon brain. Glutamate 179 in the second transmembrane domain is insufficient for strong rectification. *J. Biol. Chem.* 271:15729–15735.

Kubo, Y., and Y. Murata. 2001. Control of rectification and permeation by two distinct sites after the second transmembrane region in Kir2.1 K^+ channel. *J. Physiol.* 531:645–660.

Kubo, Y., E. Reuveny, P.A. Slesinger, Y.N. Jan, and L.Y. Jan. 1993b. Primary structure and functional expression of a rat G-protein-coupled muscarinic potassium channel. *Nature.* 364:802–806.

Kubo, Y., M. Yoshimichi, and S.H. Heinemann. 1998. Probing pore topology and conformational changes of Kir2.1 potassium channels by cysteine scanning mutagenesis. *FEBS Lett.* 435:69–73.

Lesage, F., F. Duprat, M. Fink, E. Guillemare, T. Coppola, M. Lazdunski, and J.P. Hugnot. 1994. Cloning provides evidence for a family of inward rectifier and G-protein coupled K^+ channels in the brain. *FEBS Lett.* 353:37–42.

Lopatin, A.N., E.N. Makhina, and C.G. Nichols. 1994. Potassium channel block by cytoplasmic polyamines as the mechanism of intrinsic rectification. *Nature.* 372:366–369.

Lopatin, A.N., E.N. Makhina, and C.G. Nichols. 1995. The mechanism of inward rectification of potassium channels: "long-pore plugging" by cytoplasmic polyamines. *J. Gen. Physiol.* 106:923–955.

Lu, T., B. Nguyen, X. Zhang, and J. Yang. 1999. Architecture of a K^+ channel inner pore revealed by stoichiometric covalent modification. *Neuron.* 22:571–580.

Lu, Z., and R. MacKinnon. 1994. Electrostatic tuning of Mg^{2+} affinity in an inward-rectifier K^+ channel. *Nature.* 371:243–246.

Matsuda, H. 1988. Open-state substructure of inwardly rectifying potassium channels revealed by magnesium block in guinea-pig heart cells. *J. Physiol.* 397:237–258.

Matsuda, H., A. Saigusa, and H. Irisawa. 1987. Ohmic conductance through the inwardly rectifying K channel and blocking by internal Mg^{2+}. *Nature.* 325:156–159.

Minor, D.L., Jr., S.J. Masseling, Y.N. Jan, and L.Y. Jan. 1999. Transmembrane structure of an inwardly rectifying potassium channel. *Cell.* 96:879–891.

Nichols, C.G., and A.N. Lopatin. 1997. Inward rectifier potassium channels. *Annu. Rev. Physiol.* 59:171–191.

Niwa, H., K. Yamamura, and J. Miyazaki. 1991. Efficient selection for high-expression transfectants with a novel eukaryotic vector. *Gene.* 108:193–199.

Oishi, K., K. Omori, H. Ohyama, K. Shingu, and H. Matsuda. 1998. Neutralization of aspartate residues in the murine inwardly rectifying K^+ channel IRK1 affects the substate behaviour in Mg^{2+} block. *J. Physiol.* 510:675–683.

Pearson, W.L., and C.G. Nichols. 1998. Block of the Kir2.1 channel pore by alkylamine analogues of endogenous polyamines. *J. Gen. Physiol.* 112:351–363.

Sabirov, R.Z., T. Tominaga, A. Miwa, Y. Okada, and S. Oiki. 1997. A conserved arginine residue in the pore region of an inward rectifier K channel (IRK1) as an external barrier for cationic blockers. *J. Gen. Physiol.* 110:665–677.

Stanfield, P.R., N.W. Davies, P.A. Shelton, M.J. Sutcliffe, I.A. Khan, W.J. Brammar, and E.C. Conley. 1994. A single aspartate residue is involved in both intrinsic gating and blockage by Mg^{2+} of the inward rectifier, IRK1. *J. Physiol.* 478:1–6.

Taglialatela, M., E. Ficker, B.A. Wible, and A.M. Brown. 1995. C-terminus determinants for Mg^{2+} and polyamine block of the inward rectifier K^+ channel IRK1. *EMBO J.* 14:5532–5541.

Takumi, T., T. Ishii, Y. Horio, K. Morishige, N. Takahashi, M. Yamada, T. Yamashita, H. Kiyama, K. Sohmiya, S. Nakanishi, et al. 1995. A novel ATP-dependent inward rectifier potassium channel expressed predominantly in glial cells. *J. Biol. Chem.* 270: 16339–16346.

Thompson, G.A., M.L. Leyland, I. Ashmole, M.J. Sutcliffe, and P.R. Stanfield. 2000. Residues beyond the selectivity filter of the K^+ channel kir2.1 regulate permeation and block by external Rb^+ and Cs^+. *J. Physiol.* 526(Pt 2):231–240.

Vandenberg, C.A. 1987. Inward rectification of a potassium channel in cardiac ventricular cells depends on internal magnesium ions. *Proc. Natl. Acad. Sci. USA.* 84:2560–2564.

Wible, B.A., M. Taglialatela, E. Ficker, and A.M. Brown. 1994. Gating of inwardly rectifying K^+ channels localized to a single negatively charged residue. *Nature.* 371:246–249.

Xie, L.H., S.A. John, and J.N. Weiss. 2002. Spermine block of the strong inward rectifier potassium channel Kir2.1: dual roles of surface charge screening and pore block. *J. Gen. Physiol.* 120:53–66.

Yang, J., Y.N. Jan, and L.Y. Jan. 1995. Control of rectification and permeation by residues in two distinct domains in an inward rectifier K^+ channel. *Neuron.* 14:1047–1054.